Neutrino Tomography of the Earth with ORCA Detector

S. T. Petcov

SISSA/INFN, Trieste, Italy, and
Kavli IPMU, University of Tokyo, Japan

International Workshop on
Multi-Messenger Tomography of Earth (MMTE 2022)
Snowbird, Utah, USA, July 31, 2022

Based on: F. Capozzi and S.T.P., EPJ C82 (2022) 461 [arXiv:2111.13048]

Research in Neutrino Physics: we strive to understand at deepest level what are the origins of neutrino masses and mixing and what determines the pattern of neutrino mixing and of neutrino mass squared differences that emerged from the neutrino oscillation data in the recent years. And we try to understand what are the implications of the remarkable discovery that neutrinos have mass, mix and oscillate for elementary particle physics, cosmology and for better understanding of the Earth, the Sun, the stars, formation of Galaxies, the Early Universe, i.e., for better deeper understanding of Nature in general.

The Earth

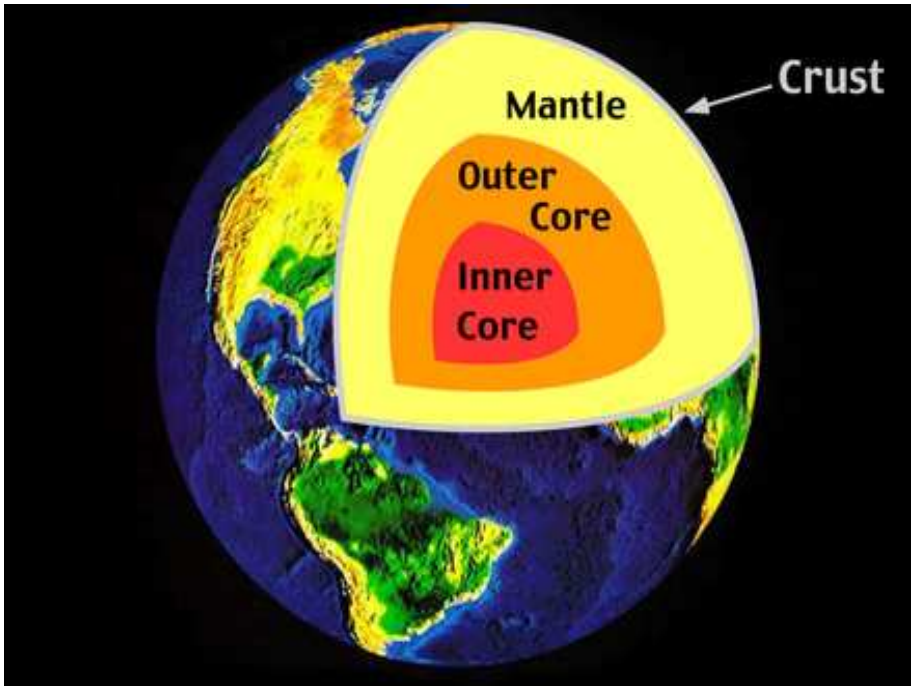

he ORCA proposed detector

Multi-PMT DOM
31 small PMTs
Almost uniform coverage
Photon counting
Direction of photon
All electronics inside

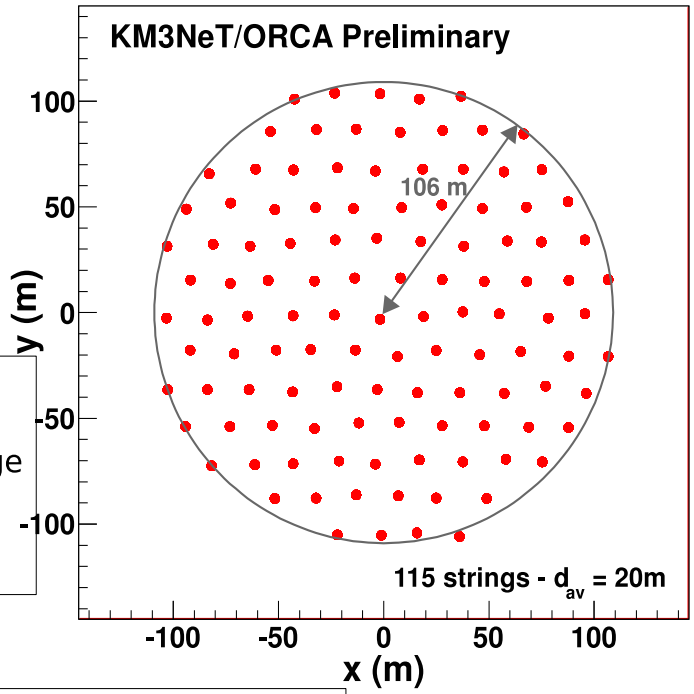

115 strings (building block) of 18 DOMs each
Estimated cost 40M€

ORCA detector - part of the KM3Net Project. Located in the Mediterranean sea 40 km off the coast of Toulon, France. Letter of Intent: arXiv:1601.07459; we use the "benchmark configuration" of ORCA (9 m vertical spacing betweem DOMs). 6 strings (length of 150 m) out of 115 planned with spacing of 20 m installed and provide data. The total instrumented volume of ORCA will be $\sim$ 3.7 Mton of sea water; $E_\nu \gtrsim$ 2 GeV.

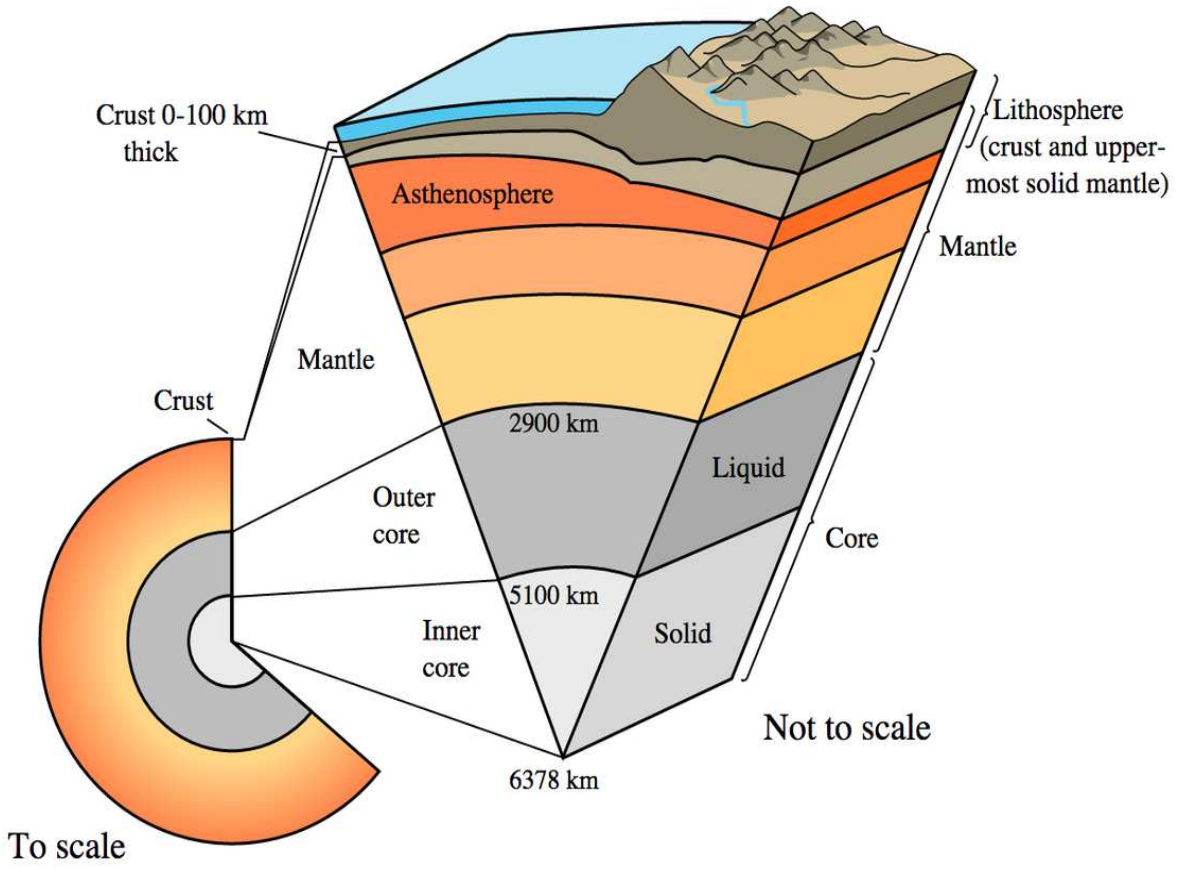
Crust 0-100 km
thick
Lithosphere
(crust and upper-
most solid mantle)
Asthenosphere
Mantle
Mantle
Crust
2900 km
Liquid
Outer
core
Core
5100 km
Inner
core
Solid
Not to scale
6378 km
To scale

At present our knowledge about the interior composition of the Earth and its density structure is based primarily on seismological and geophysical data.

See, e.g., W.F. McDonough, "Treatise on Geochemistry: The Mantle and Core", vol. 2 (ed. R. W. Carlson, Elsevier-Pergamon, Oxford, 2003), p. 547.
B.L.N. Kennett, Geophys. J. Int. **132**, 374 (1998);
G. Masters and D. Gubbins, Phys. Earth Planet. Inter. **140**, 159 (2003).

These data were used to construct the Preliminary Reference Earth Model (PREM) of the density distribution of the Earth: A. M. Dziewonski and D. L. Anderson, "Preliminary reference earth model," Phys. Earth Planet. Interiors 25 (1981) 297.

In the PREM model, $\rho_{\rm E}$ is assumed to be spherically symmetric, $\rho_{\rm E} = \rho_{\rm E}(r)$, r being the distance from the Earth center, and there are two major density structures - the core and the mantle, and a certain number of substructures (shells or layers). The mantle has seven shells in the model, while the core is divided into an Inner Core (IC) and Outer Core (OC).

The change of $\rho_{\rm E}$ (N_e) from the mantle to the core, according to PREM, can well be approximated by a step function.

The Earth (PREM)

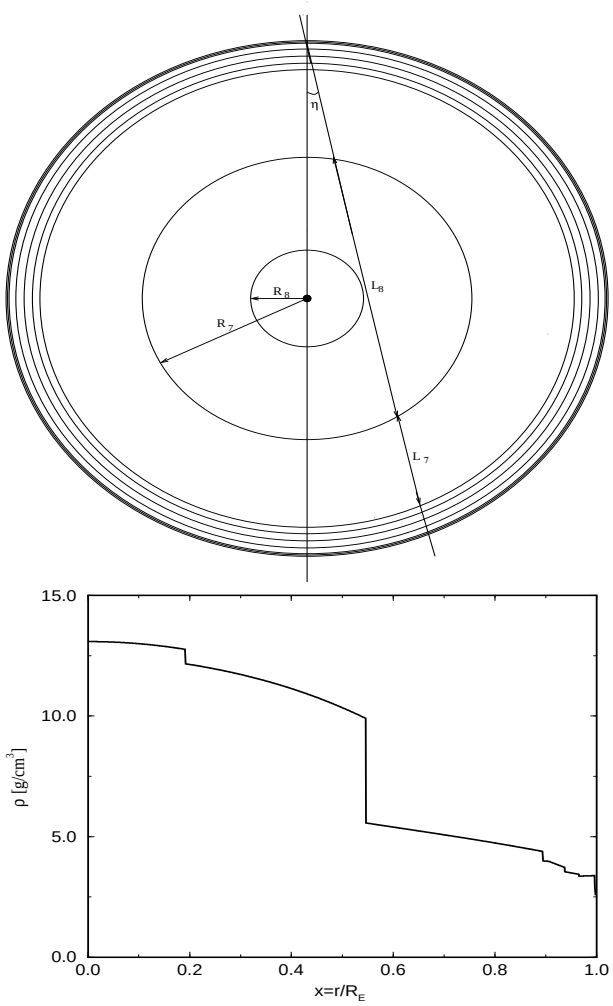

FIG. 1. Density profile of the Earth.

$R_\oplus = 6371$ km; $R_{\rm IC} = 1221.5$ km; $R_{\rm C} = 3480$ km; $D_{\rm man} = 2891$ km;
$\bar{\rho}_{\rm man} = 4.45$ g/cm^3; $\bar{\rho}_{\rm C} = 10.99$ g/cm^3; $\bar{\rho}_{\rm IC} = 12.89$ g/cm^3; $\bar{\rho}_{\rm OC} = 10.90$ g/cm^3.

Spherically symmetric ρ_{E}: the ν trajectory through the Earth is specified by the nadir (zenith) angle θ_n (or θ_z).

For $\theta_n \leq 33.17^o$, or path lengths $L \geq 10660$ km, neutrinos cross the Earth core.

The path length for neutrinos which cross only the Earth mantle is given by $L = 2R_\oplus \cos\theta_n$, θ_n.

If neutrinos cross the Earth core, the lengths of the paths in the mantle, $2L^{\mathsf{man}}$, and in the core, L^{core}, are determined by: $L^{\mathsf{man}} = R_\oplus \cos\theta_n - (R_c^2 - R_\oplus^2 \sin^2\theta_n)^{\frac{1}{2}}$, $L^{\mathsf{core}} = 2(R_c^2 - R_\oplus^2 \sin^2\theta_n)^{\frac{1}{2}}$.

$\rho_{\mathsf{E}}(r)$ (N_e) changes relatively little around the quoted mean values along the trajectories of neutrinos which cross a substantial part of the Earth mantle, or the mantle, the outer core and the inner core.

The determination of the radial density distributions in the mantle and core, $\rho_{man}(r)$ and $\rho_c(r)$, from seismological and geophysical data is not direct and suffers from uncertainties.

B. A. Bolt, Q. J. R. Astron. Soc. **32**, 367 (1991).
B.L.N. Kennett, Geophys. J. Int. **132**, 374 (1998);
G. Masters and D. Gubbins, Phys. Earth Planet. Inter. **140**, 159 (2003).

It requires the knowledge, in particular, of the seismic wave speed velosity distribution in the interrior of the Earth, which depends on the pressure, tempertaure, composition and elastic properties of the Earth's interior that are not known with a good/high precision.
Often $\rho_{\rm E}(r)$ is determined using an empirical relation between the seismic wave velosities and $\rho_{\rm E}(r)$ (one example is the Birch low, which may fail at the higher densities of the core) and the so-called "Adams-Williamson eqaution" (from 1923). E. Williamson and L.H. Adams, J. Wash. Acad. Sci. 13 (1923) 413.

An approximate and perhaps rather conservative estimate of this uncertainty for $\rho_{\rm man}(r)$ is $\sim 5\%$; for the core density $\rho_c(r)$ it is larger and can be significantly larger (Bolt:1991,Kennett:1998,Masters:2003).

A precise knowledge of $\rho_{\mathrm{E}}(r)$ and of $\bar{\rho}_{\mathrm{man}}$, $\bar{\rho}_{\mathrm{C}}$ and $\bar{\rho}_{\mathrm{IC}}$, is essential for understanding the physical conditions and fundamental aspects of the structure and properties of the Earth's interior
(including the dynamics of mantle and core,
the bulk composition of the Earth's three structures,
the generation, properties and evolution of the Earth's magnetic field and the gravity field of the Earth)
(Bolt:1991,Yoder:1995,McDonough:2003,McDonough:2008zz).

The thermal evolution of the Earth's core, in particular, depends critically on the density change across the inner core - outer core boundary (see, e.g., Baffet:1991).

An independent determination of $\rho_{\mathrm{E}}(r)$ and of $\bar{\rho}_{\mathrm{man}}$, $\bar{\rho}_{\mathrm{C}}$ and $\bar{\rho}_{\mathrm{IC}}$, is highly desirable and would be extremely useful.

A unique alternative method of determination of the density profile of the Earth is the neutrino tomography of the Earth.

The propagation of the active flavour neutrinos and antineutrinos ν_α and $\bar{\nu}_\alpha$, $\alpha = e, \mu, \tau$, in the Earth is affected by the Earth matter.

The original idea is based on the observation that
$\sigma(\nu_\alpha(\bar{\nu}_\alpha) + N)$ rises with energy.
For ν_α, $\bar{\nu}_\alpha$ with $E_\nu \gtrsim$ a few TeV, the inelastic scattering off protons and neutrons leads to absorption of νs and thus to attenuation of the initial ν flux.
The magnitude of the attenuation depends on the Earth matter density profile along the neutrino path.
Attenuation data for νs with different path-lengths in the Earth carry information about the matter density distribution in the Earth interior.
The absorption method of Earth tomography with accelerator neutrino beams, which is difficult (if not impossible) to realise in practice , was discussed first by Placci and Zavattini in 1973 and Volkova and Zatsepin in 1974, and later in grater detail in Nedyalkov:1981, Nedyalkov:1981yy, Nedyalkov:1982, Nedyalkov:1983, DeRujula:1983ya, Wilson:1983an, Askar:1984, Borisov:1986sm, Borisov:1989kh, Winter:2006vg, Kuo95, Jain:1999kp, Reynoso:2004dt.

Atmospheric νs are a perfect tool for performing Earth tomography:
i) consist of significant fluxes of ν_μ, ν_e, $\bar{\nu}_\mu$ and $\bar{\nu}_e$, produced in the interactions of cosmic rays with the Earth atmosphere,
ii) have a wide range of energies spanning the interval from a few MeV to multi-GeV to multi-TeV,
iii) being produced isotropically in the upper part of the Earth atmosphere at a height of ~ 15 km, they travel distances from ~ 15 km to 12742 km before reaching detectors located on the Earth surface, crossing the Earth along all possible directions and thus "scanning" the Earth interior.

See, e.g., T.K. Gaisser and M. Honda, Ann. Rev. Nucl. Part. Sci. **52** (2002) 153 [arXiv:hep-ph/0203272]

The interaction rates that allow to get information about the Earth density distribution can be obtained in the currently taking data IceCube experiment and in the future experiments PINGU, ORCA (within KM3Net project), Hyper Kamiokande and DUNE, which are under construction.

Atmospheric neutrinos

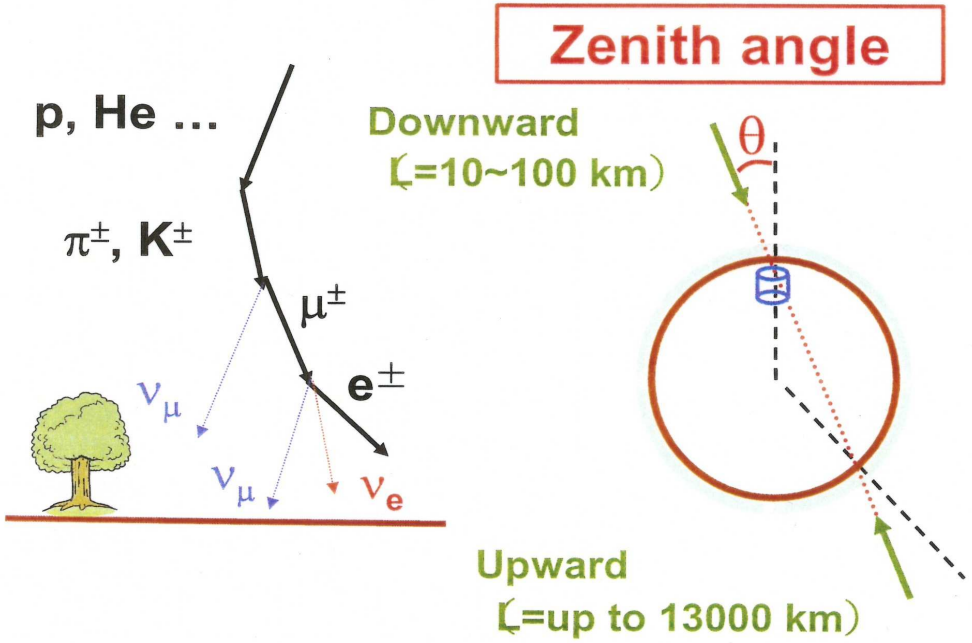

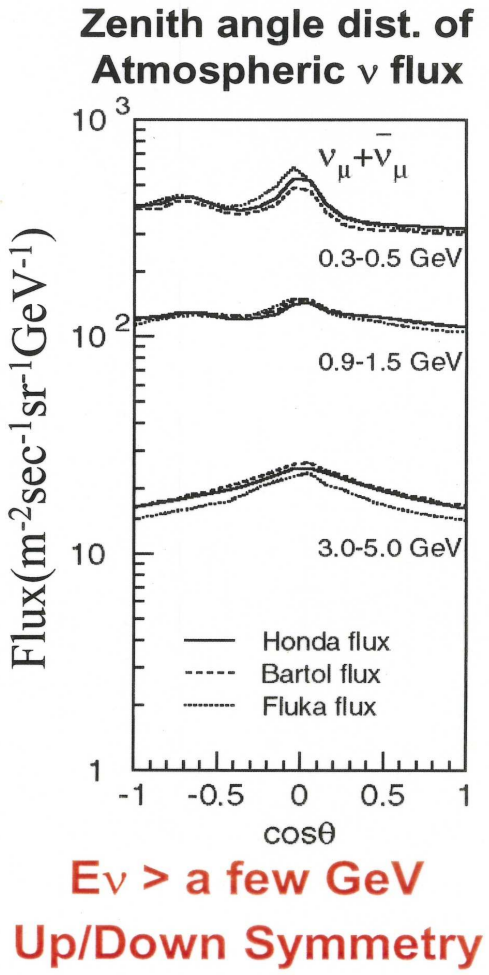

Eν > a few GeV

Up/Down Symmetry

Neutrino Oscillation Source

- Northern Hemisphere ν_μ oscillating over one earth radii produces ν_μ (ν_τ) oscillation minimum(maximum) at ~25 GeV
  - Covers all possible terrestrial baselines
  - "Beam" is free and never turns off

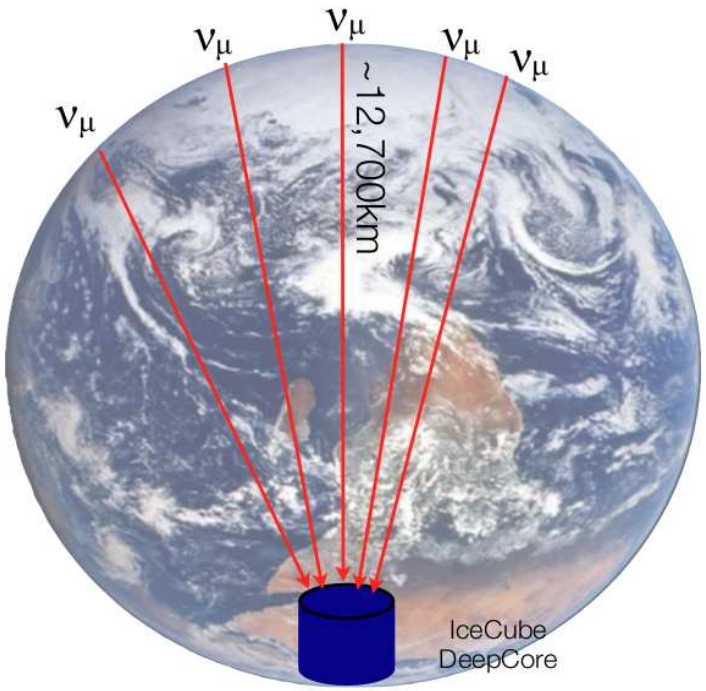

Mena, Mociou & Razzaque, *Phys. Rev.* D**78**, 093003 (2008)

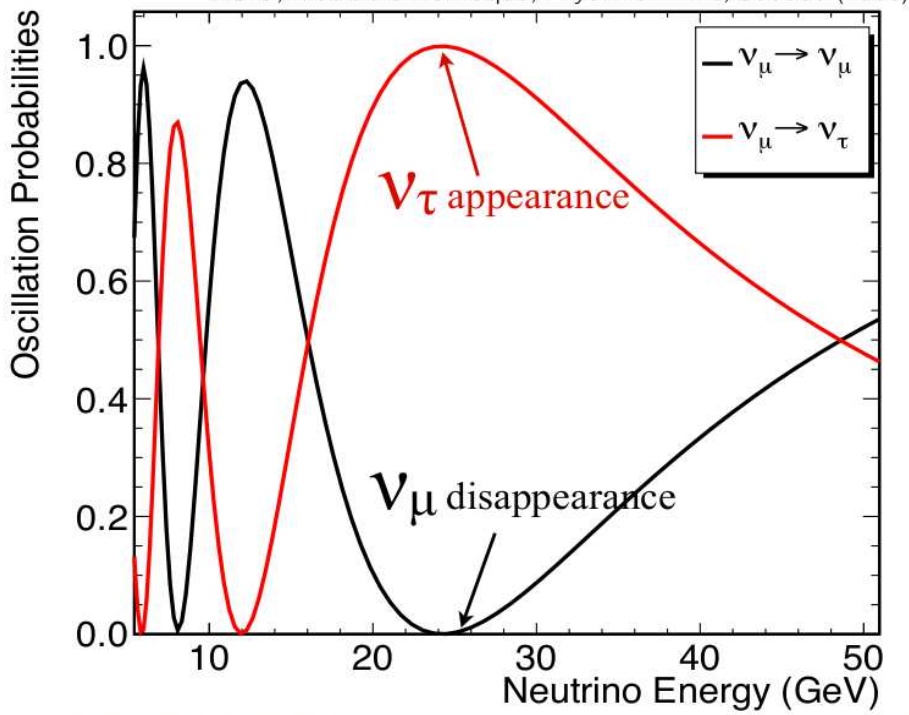

The idea of using the absorption method of Earth tomography with atmospheric neutrinos was discussed first in
M. C. Gonzalez-Garcia *et al.*, Phys. Rev. Lett. 100 (2008) 061802.

A. Donini, S. Palomares-Ruiz and J. Salvado, Nature Phys. 15 (2019) 37, using the IceCube zenith angle distribution data on multi-TeV (1.5-20.0 TeV) atmospheric ν_μ and $\bar{\nu}_\mu$ obtained information about $\rho_{\rm E}(r)$, which, although not very precise, broadly agrees with the PREM model.

"Weighted" the Earth with neutrinos: $M^\nu_\oplus = (6.0^{+1.6}_{-1.3}) \times 10^{24}$ kg,
to be compared with the gravitationally determined value:
$M_\oplus = (5.9722 \pm 0.0006) \times 10^{24}$ kg.

Marked the beginning of real experimental data driven neutrino tomography of the Earth.

The oscillations $\nu_\alpha \leftrightarrow \nu_\beta$ and $\bar{\nu}_\alpha \leftrightarrow \bar{\nu}_\beta$, $\alpha, \beta = e, \mu$, having $E \sim (0.1 - 15.0)$ GeV and traversing the Earth can be strongly modified by the Earth matter effects. These modifications depend on the Earth matter density (more precisely, the electron number density $N_e(r)$, see further) along the path of the νs. Thus, by studying the effects of Earth matter on the oscillations of, e.g., ν_μ and ν_e ($\bar{\nu}_\mu$ and $\bar{\nu}_e$) neutrinos traversing the Earth along different trajectories it is possible to obtain information about the Earth (electron number) density distribution.

Neutrino Oscillations in Matter (Earth mantle)

When neutrinos propagate in matter, they interact with the backgrpound of electrons, protons and neutrnos, which generates an effective potential in the neutrino Hamiltonian: $H = H_{vac} + V_{eff}$.

This modifies the neutrino mixing since the eigenstates and the eigenvalues of H_{vac} and of $H = H_{vac} + V_{eff}$ are different, leading to a different oscillation probability w.r.t to that in vacuum.

Typically the matter background is not CP and CPT symmetric, e.g., the Earth and the Sun contain only electrons, protons and neutrons, and the resulting oscillations violate CP and CPT symmetries.

$$P_{3\nu}(\nu_\mu \to \nu_e) \cong \sin^2\theta_{23}\,\sin^2 2\theta^m_{13}\,\sin^2\frac{\Delta M^2_{31} L}{4E}$$

$\sin^2 2\theta^m_{13}$, ΔM^2_{31} depend on the matter potential $V_{eff} = \sqrt{2}\, G_F\, N_e$,

For antineutrinos V_{eff} has the opposite sign: $V_{eff} = -\sqrt{2}\, G_F, N_e$.

$\Delta m^2_{31} > 0$ (NO): $\nu_{\mu(e)} \to \nu_{e(\mu)}$ matter enhanced, $\bar{\nu}_{\mu(e)} \to \bar{\nu}_{e(\mu)}$ - suppressed

$\Delta m^2_{31} < 0$ (IO): $\bar{\nu}_{\mu(e)} \to \bar{\nu}_{e(\mu)}$ matter enhanced, $\nu_{\mu(e)} \to \nu_{e(\mu)}$−suppressed

$$\sin^2 2\theta_{13}^m = \frac{\tan^2 2\theta_{13}}{(1-\frac{N_e}{N_e^{res}})^2+\tan^2 2\theta_{13}},$$

$$\cos 2\theta_{13}^m = \frac{1-N_e/N_e^{res}}{\sqrt{(1-\frac{N_e}{N_e^{res}})^2+\tan^2 2\theta_{13}}},$$

$$N_e^{res} = \frac{\Delta m^2_{31}\cos 2\theta_{13}}{2E\sqrt{2}G_F} \cong$$

$$6.56\times 10^6\,\frac{\Delta m^2[\mathrm{eV}^2]}{E[\mathrm{MeV}]}\cos 2\theta\,\mathrm{cm}^{-3}\ \mathrm{N_A}\,,$$

$$\frac{\Delta M^2_{31}}{2E} \equiv \frac{\Delta m^2_{31}}{2E}\left((1-\frac{N_e}{N_e^{res}})^2\cos^2 2\theta_{13}+\sin^2 2\theta_{13}\right)^{\frac{1}{2}}$$

For $\bar\nu_\mu \to \bar\nu_e$: $N_e \to (-N_e)$.

Earth matter effect in $\nu_\mu \to \nu_e$, $\bar{\nu}_\mu \to \bar{\nu}_e$ in the mantle (MSW)

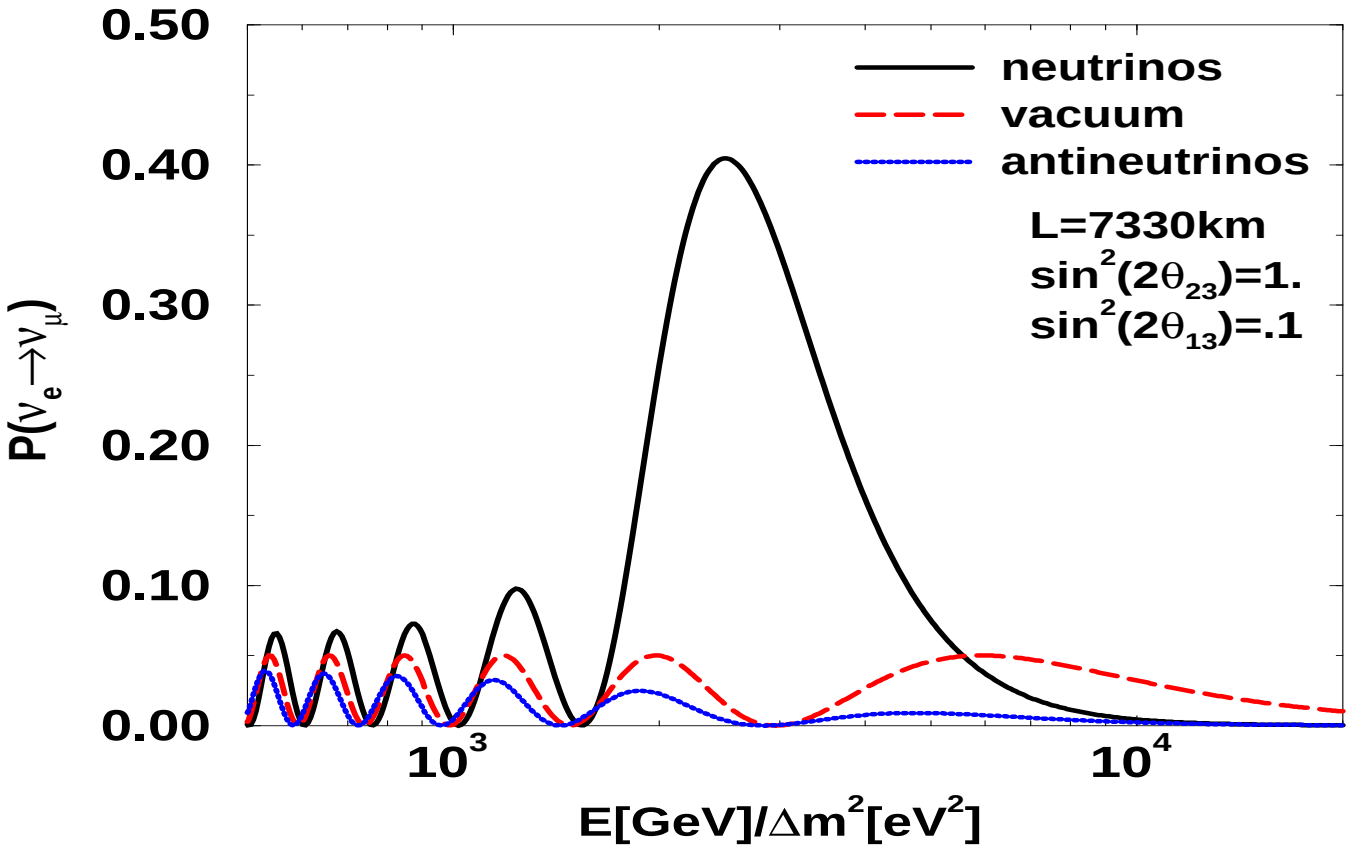

$\Delta m^2_{31} = 2.5 \times 10^{-3}$ eV^2, $E^{res} = 6.25$ GeV; $P^{3\nu} = \sin^2\theta_{23} P^{2\nu}_m = 0.5 P^{2\nu}_m$;
$N^{res}_e \cong 2.3$ cm^{-3} N$_A$; $L^{res}_m = L^v/\sin 2\theta_{13} \cong 6250/0.32$ km; $2\pi L/L_m \cong 0.75\pi (\neq \pi)$.

I. Mocioiu, R. Shrock, 2000

Oscillations of Neutrinos Crossing the Earth Core

Resonance-like Amplification of Oscillations of Neutrinos Crossing the Earth Core

Earth matter effects in $\nu_\mu \to \nu_e$, $\bar{\nu}_\mu \to \bar{\nu}_e$ (NOLR)

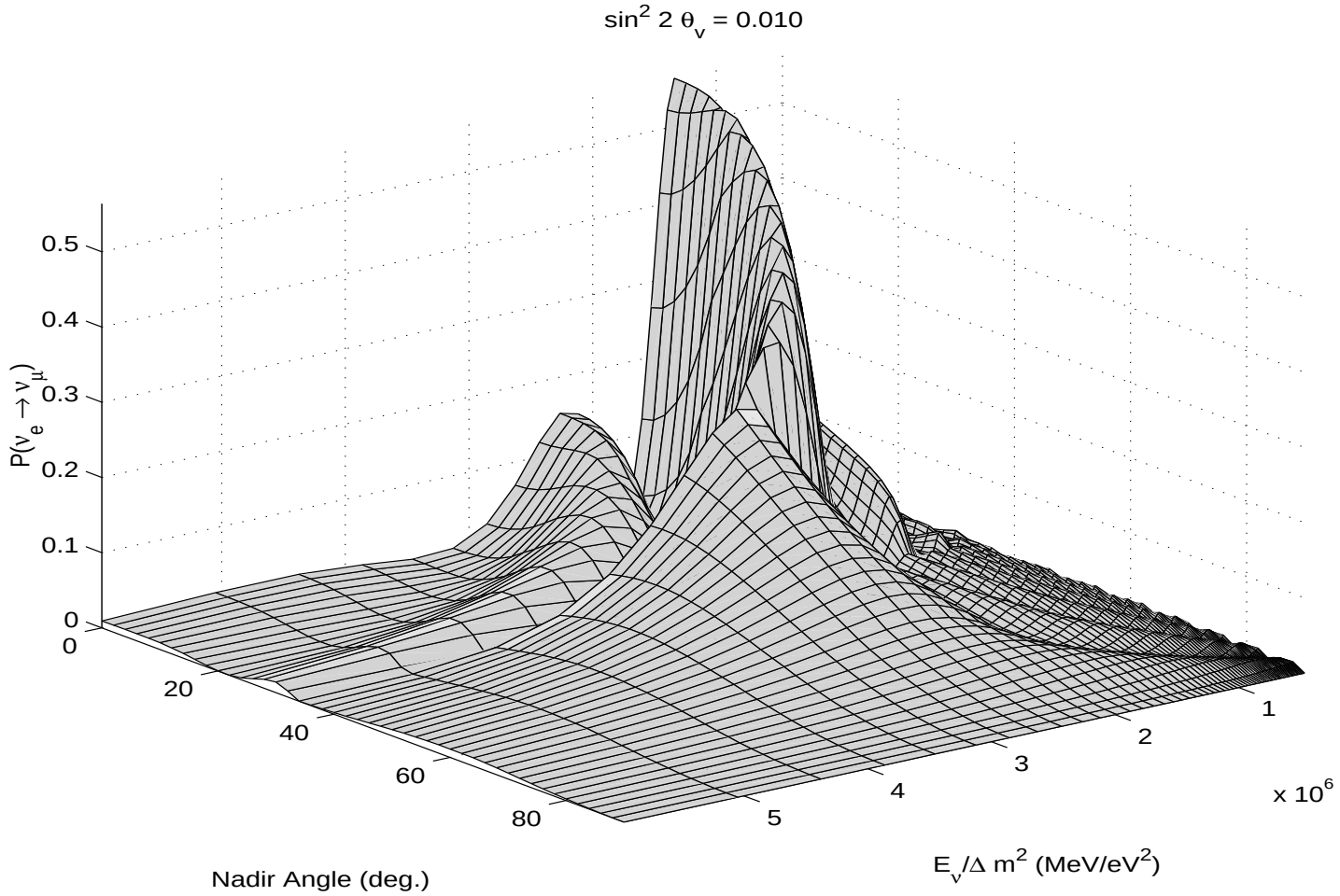

S.T.P., 1998;
M. Chizhov, M. Maris, S.T.P., 1998; M. Chizhov, S.T.P., 1999

$P(\nu_e \to \nu_\mu) \equiv P_{2\nu} \equiv (s_{23})^{-2} P_{3\nu}(\nu_{e(\mu)} \to \nu_{\mu(e)})$, $\theta_{\rm v} \equiv \theta_{13}$, $\Delta m^2 \equiv \Delta m^2_{\rm atm}$;
Absolute maximum: Neutrino Oscillation Length Resonance (NOLR);
Local maxima: MSW effect in the Earth mantle or core.

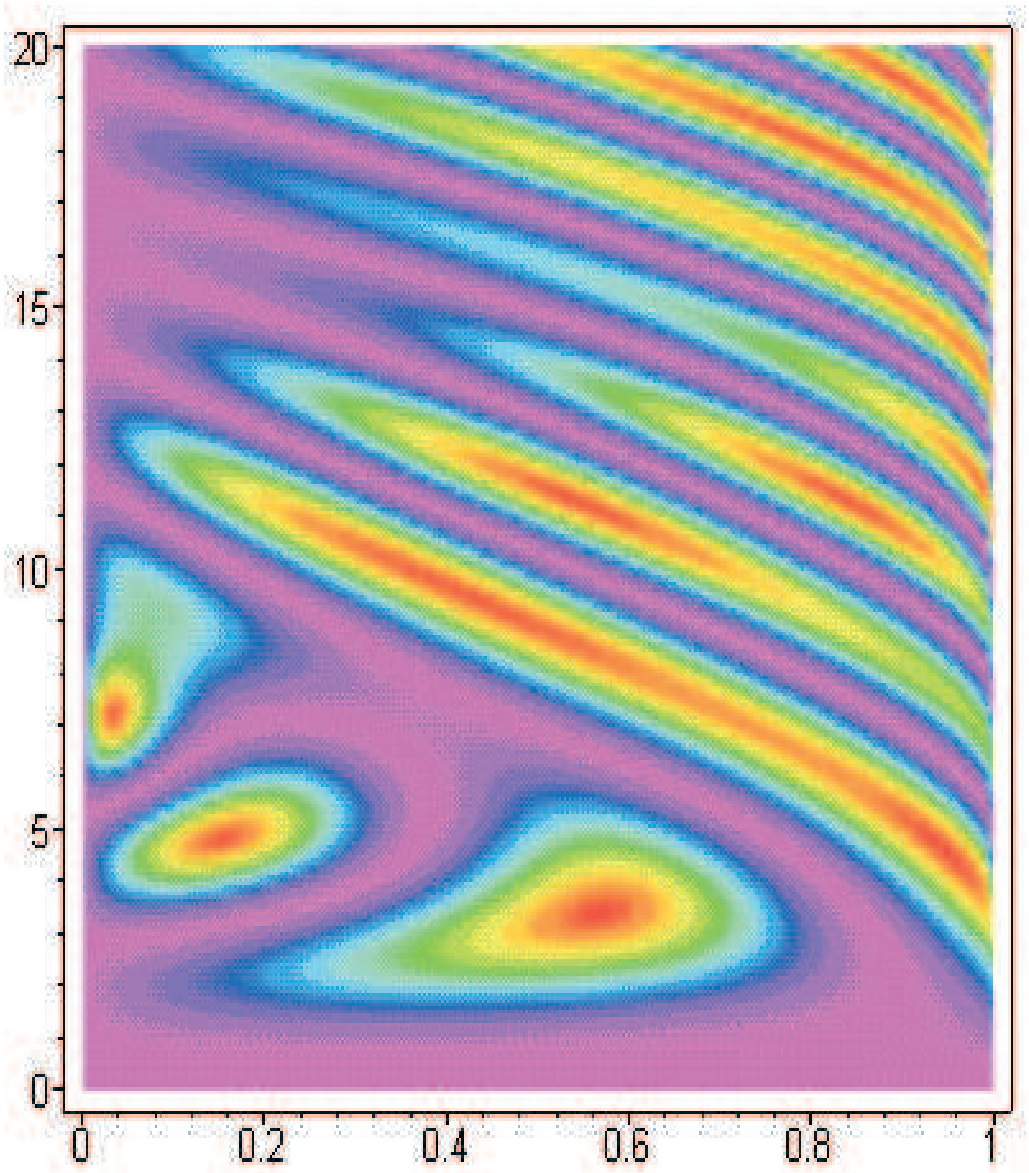

$(s_{23})^{-2} P_{3\nu}(\nu_{e(\mu)} \to \nu_{\mu(e)}) \equiv P_{2\nu}$; **NOLR: "Dark Red Spots"**, $P_{2\nu} = 1$;
Vertical axis: $\Delta m^2/E$ $[10^{-7} eV^2/MeV]$; **horizontal axis:** $\sin^2 2\theta_{13}$; $\theta_n = 0$

M. Chizhov, S.T.P., 1999 (hep-ph/9903399,9903424)

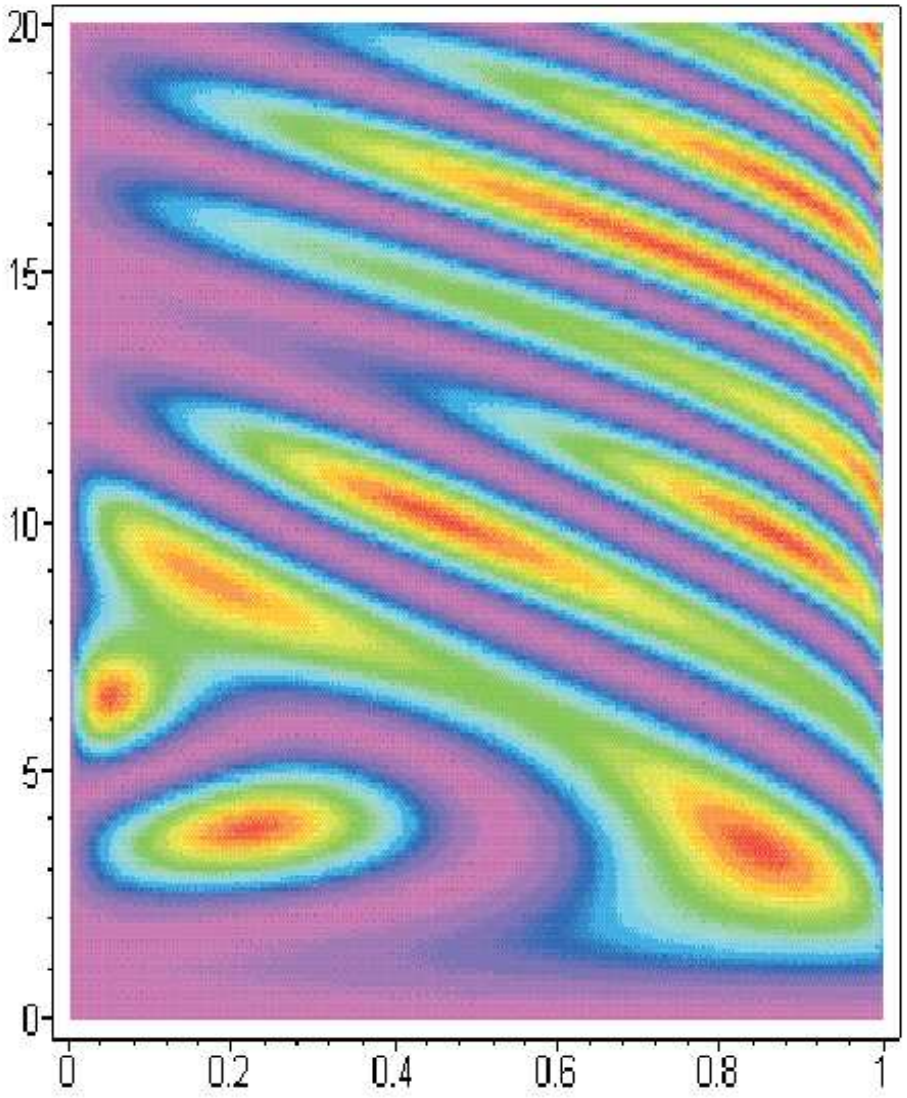

The same for $\theta_n = 23^\circ$.
Vertical axis: $\Delta m^2/E$ $[10^{-7} eV^2/MeV]$; horizontal axis: $\sin^2 2\theta_{13}$.

M. Chizhov, S.T.P., 1999 (hep-ph/9903399,9903424)

• **For Earth center crossing ν's ($\theta_n = 0$) and, e.g. $\sin^2 2\theta_{13} = 0.01$, NOLR occurs at $E \cong 4$ GeV ($\Delta m^2(atm) = 2.5 \times 10^{-3}$ eV^2).**

S.T.P., hep-ph/9805262

• **For the Earth core crossing ν's: $P_{2\nu} = 1$ due to NOLR when**

$$\tan \Phi^{\text{man}}/2 \equiv \tan \phi' = \pm \sqrt{\frac{-\cos 2\theta''_m}{\cos(2\theta''_m - 4\theta'_m)}},$$

$$\tan \Phi^{\text{core}}/2 \equiv \tan \phi'' = \pm \frac{\cos 2\theta'_m}{\sqrt{-\cos(2\theta''_m)\cos(2\theta''_m - 4\theta'_m)}}$$

Φ^{man} (Φ^{core}) - phase accumulated in the Earth mantle (core), θ'_m (θ''_m) - the mixing angle in the Earth mantle (core).

$P_{2\nu} = 1$ due to NOLR for $\theta_n = 0$ (Earth center crossing ν's) at, e.g. $\sin^2 2\theta_{13} = 0.034;\ 0.154$, $E \cong 3.5;\ 5.2$ GeV ($\Delta m^2(atm) = 2.5 \times 10^{-3}$ eV^2).

At the same time for E =3.5 GeV (5.2 Gev), the probability $P_{2\nu} \gtrsim 0.5$ for the values of $\sin^2 2\theta_{13}$ from the interval $0.02 \lesssim \sin^2 2\theta_{13} \lesssim 0.10$ ($0.04 \lesssim \sin^2 2\theta_{13} \lesssim 0.26$).

M. Chizhov, S.T.P., Phys. Rev. Lett. 83 (1999) 1096 (hep-ph/9903399); Phys. Rev. Lett. 85 (2000) 3979 (hep-ph/0504247); Phys. Rev. D63 (2001) 073003 (hep-ph/9903424).

The Earth matter effects in $\nu_{e(\mu)} \to \nu_{\mu(e)}$, $\bar{\nu}_{e(\mu)} \to \bar{\nu}_{\mu(e)}$, $\nu_e \to \nu_\tau$ and $\bar{\nu}_e \to \bar{\nu}_\tau$ oscillations are significant for $E_\nu \sim (2 - 10)$ GeV.

The mantle-core (NOLR) enhancement of $P_m^{2\nu}$ (or $\bar{P}_m^{2\nu}$) is relevant, in particular, for the searches of sub-dominant $\nu_{e(\mu)} \to \nu_{\mu(e)}$ (or $\bar{\nu}_{e(\mu)} \to \bar{\nu}_{\mu(e)}$) oscillations of atmospheric neutrinos having energies $E \gtrsim 2$ GeV and crossing the Earth core on the way to the detector.

S.T.P., hep-ph/9805262; M. Chizhov, S.T.P., hep-ph/9903424

The effects of Earth matter on the oscillations of atmospheric (and accelerator) neutrinos have not been observed so far; can be used for performing tomography of the Earth with neutrinos having $E_\nu \sim (2 - 10)$ GeV.

The fluxes of atmospheric $\nu_{e,\mu}$ of energy E, which reach the detector after crossing the Earth along a given trajectory specified by the value of θ_n, $\Phi_{\nu_{e,\mu}}(E,\theta_n)$, are given by the following expressions in the case of the 3-neutrino oscillations under discussion:

$$\Phi_{\nu_e}(E,\theta_n) \cong \Phi^0_{\nu_e}\left(1 + [s^2_{23}r - 1]\ P^{2\nu}_m\right),$$

$$\Phi_{\nu_\mu}(E,\theta_n) \cong \Phi^0_{\nu_\mu}\left(1 + s^4_{23}[(s^2_{23}\ r)^{-1} - 1]P^{2\nu}_m - 2c^2_{23}s^2_{23}\left[1 - Re\ (e^{-i\kappa}A^{2\nu}_m(\nu_\tau \to \nu_\tau))\right]\right),$$

where $\Phi^0_{\nu_{e(\mu)}} = \Phi^0_{\nu_{e(\mu)}}(E,\theta_n)$ is the $\nu_{e(\mu)}$ flux in the absence of neutrino oscillations and

$$r \equiv r(E,\theta_n) \equiv \frac{\Phi^0_{\nu_\mu}(E,\theta_n)}{\Phi^0_{\nu_e}(E,\theta_n)} \quad .$$

s^2_{23}: b.f.v. 0.573 (0.575) NO (IO); 3σ CL: (0.415-0.619).

$r(E,\theta_n) \cong (2.6 \div 4.5)$ for neutrinos giving the main contribution to the multi-GeV samples, $E \cong (2 \div 10)$ GeV.

M. Honda, 1995.

Hyper Kamiokande (5SK), IceCube-PINGU, ANTARES-ORCA;

Iron Magnetised detector: INO

INO: 50 or 100 kt (in India); ν_μ and $\bar{\nu}_\mu$ induced events detected (μ^+ and μ^-);
not designed to detect ν_e and $\bar{\nu}_e$ induced events.

IceCube at the South Pole: PINGU

PINGU: 50SK; ν_μ and $\bar{\nu}_\mu$ induced events detected (μ^+ and μ^-, no μ charge identification); Challenge: $E_\nu \gtrsim 2$ GeV (?)

KM3Net in Mediteranian sea: ORCA (near Toulon)

Studies of atmospheric ν oscillations with DUNE.

Atmospheric ν experiments

Subdominant $\nu_{\mu(e)} \to \nu_{e(\mu)}$ and $\bar{\nu}_{\mu(e)} \to \bar{\nu}_{e(\mu)}$ oscillations in the Earth.

$$P_{3\nu}(\nu_e \to \nu_\mu) \cong P_{3\nu}(\nu_\mu \to \nu_e) \cong s^2_{23}\, P_{2\nu}\,, P_{3\nu}(\nu_e \to \nu_\tau) \cong c^2_{23}\, P_{2\nu}\,,$$
$$P_{3\nu}(\nu_\mu \to \nu_\mu) \cong 1 - s^4_{23}\; P_{2\nu} - 2c^2_{23}s^2_{23}\; \left[1 - Re\; (e^{-i\kappa} A_{2\nu}(\nu_\tau \to \nu_\tau))\right]\,,$$

$P_{2\nu} \equiv P_{2\nu}(\Delta m^2_{31}, \theta_{13}; E, \theta_n; N_e)$: 2-$\nu$ $\nu_e \to \nu'_\tau$ oscillations in the Earth,
$\nu'_\tau = s_{23}\,\nu_\mu + c_{23}\,\nu_\tau$; $\Delta m^2_{21} \ll |\Delta m^2_{31(32)}|$, $E_\nu \gtrsim 2$ GeV;

κ and $A_{2\nu}(\nu_\tau \to \nu_\tau) \equiv A_{2\nu}$ are known phase and 2-ν amplitude.

NO: $\nu_{\mu(e)} \to \nu_{e(\mu)}$ matter enhanced, $\bar{\nu}_{\mu(e)} \to \bar{\nu}_{e(\mu)}$ - suppressed

IO: $\bar{\nu}_{\mu(e)} \to \bar{\nu}_{e(\mu)}$ matter enhanced, $\nu_{\mu(e)} \to \nu_{e(\mu)}$–suppressed

No charge identification (SK, HK, IceCube-PINGU, ANTARES-ORCA); event rate (DIS regime): $[2\sigma(\nu_l + N \to l^- + X) + \sigma(\bar{\nu}_l + N \to l^+ + X)]/3$

Charge identification: INO; event rate (DIS regime): $\sigma(\nu_l + N \to l^- + X)$, $\sigma(\bar{\nu}_l + N \to l^+ + X)$

The Earth tomography based on the study of the effects of Earth matter on the oscillations of atmospheric neutrinos with different path-lengths in the Earth is discussed in:

W. Winter, Nucl. Phys. B 908 (2016) 250 (PINGU, ORCA; 7 layers, densities in these layers varied independently; the Earth mass and the Earth hydrostatic equilibrium constraints; systematic errors).

S. Bourret et al. [KM3NeT], J. Phys. Conf. Ser. 888 (2017) 012114 (ORCA; systematic errors not accounted for).

A. Kumar and S. Kumar Agarwalla, JHEP 08 (2021) 139 (INO).

K. J. Kelly, P. A. N. Machado, I. Martinez-Soler and Y. F. Perez-Gonzalez, JHEP 05 (2022) 187 (DUNE).

Early studies:

S. Choubey, P. Ghoshal and S.T.P., studies performed in the period 2008 - 2011 (HK, LAr), unpublished.

S. Choubey and S.T.P., studies performed in 2014 (PINGU), unpublished.

Composition of the Earth core (N_e):

C. Rott, A. Taketa and D. Bose, Sci. Rep. 5 (2015) 15225 (generic detector).

S. Bourret *et al.*, PoS ICRC2019 (2020) 1024 (ORCA).

Important Constraints

The total Earth mass constraint:

$$M_\oplus = (5.9722 \pm 0.0006) \times 10^{24} \text{ kg}$$

Earth hydrostatic equilibrium constraint:

$$\rho_{man} \leq \rho_{OC} \leq \rho_{IC}.$$

Earth momentum of inertia constraint:

$$I_\oplus = (8.01736 \pm 0.00097) \times 10^{37} \text{ kg m}^2.$$

$$I_\oplus = 0.330745\, M_\oplus\, R_\oplus^2.$$

The Earth matter effects in the ν oscillations depend on

$$V = \sqrt{2}\, G_{\mathsf{F}}\, N_e$$

$$N_e^{(E)}(r) = \rho_{\mathsf{E}}(r)\, Y_e / m_{\mathsf{N}},$$

Y_e **- electron fraction number (or** Z/A **factor).**

For isotopically symmetric matter $Y_e = 0.5$**.**

Earth core composition models: $Y_e^c = 0.466 - 0.471$**.**

Earth mantle composition models: $Y_e^{man} = 0.490 - 0.496$**.**

We used: $Y_e^{man} = 0.490$ **and** $Y_e^c = 0.467$**.**

However, varying Y_e^c **and** Y_e^{man} **in the indicated respective intervals has no effect on our results.**

Aspects of the Analysis

We change the PREM density in a given layer $\rho_i(r)$, $i = \mathrm{IC}, \mathrm{OC}, \mathrm{man}$, by a factor $(1 + \kappa_i)$, κ_i is r-independent real constant:

$$\rho_i(r) \to (1 + \kappa_i)\rho_i(r).$$

We will present results on sensitivity of ORCA to

$$\Delta\rho_i = 100\%\,((1 + \kappa_i)\rho_i(r) - \rho_i(r))/\rho_i(r) = 100\%\,\kappa_i.$$

The Earth mass constraint, i.e., $M_\oplus$ should remain unchanged when varying $\rho_i(r)$, is accounted for.

When we consider, e.g., variation of $\rho_{\mathrm{IC}}(r)$, we study two cases:
we compensate it by the corresponding change of density of i) the outer core $\rho_{\mathrm{OC}}(r)$, and ii) of the mantle $\rho_{\mathrm{man}}(r)$.
We proceed in a similar way when we analyse the sensitivity of ORCA to the OC, core and mantle densities, $\rho_{\mathrm{OC}}(r)$, $\rho_{\mathrm{C}}(r)$, and $\rho_{\mathrm{man}}(r)$.

In order to assess the effect of the Earth total mass constraint we obtained results on the ORCA's sensitivity to the mantle, outer core, inner core and total core densities without imposing this external constraint.

Simulation of Events in ORCA

For the unoscillated fluxes of atmospheric ν_μ, ν_e, and $\bar{\nu}_\mu$, $\bar{\nu}_e$, $\Phi_\alpha(\theta_n, E)$ and $\bar{\Phi}_\alpha(\theta_n, E)$, we use azimuth-averaged double differential $d^2\Phi_\alpha/(d\cos\theta_n dE)$ and $d^2\bar{\Phi}_\alpha/(d\cos\theta_n dE)$ updated fluxes from M. Honda *et al.*, arXiv:1502.0391 (i.e., the "solar minimum, without mountain over the detector" fluxes at the Frejus cite from the tables given in the web site quoted in arXiv:1502.0391).
The "source" of atmospheric neutrinos is assumed to be a layer located at 15 km above the Earth surface.

The principal observables in ORCA detector - the double differential event spectra in the neutrino energy E and nadir angle θ_n are calculated using the methods developed and described in F. Capozzi et al., arXiv:1503.01999 and arXiv:1708.03022.

The neutrino events in ORCA are divided into two classes (S. Adrian-Martinez *et al.* [KM3Net], arXiv:1601.07459): "track-like" and "cascade-like". Track-like events involve an outgoing μ^- or μ^+ and originate from charged current (CC) interactions of ν_μ, $\bar{\nu}_\mu$ and ν_τ, $\bar{\nu}_\tau$. Cascade-like events result from CC interactions of ν_e, $\bar{\nu}_e$ and ν_τ, $\bar{\nu}_\tau$, and from neutral current interactions and consist of hadronic and electromagnetic showers.

The ORCA "Letter of Intent" arXiv:1601.07459 contains estimates of the probabilities of flavour-misidentification as well as of identifying the τ and

the neutral current events as track or cascade events. We included this information from arXiv:1601.07459 in our analysis.

The relevant detection characteristics of ORCA - the energy and angular resolutions and the dependence of the effective volumes for the different types/classes of events on the initial neutrino energy - are taken from S. Adrian-Martinez *et al.* [KM3Net], arXiv:1601.07459, and correspond to the benchmark (9 m vertical spacing) configuration of ORCA.

We consider $E \in [2, 100]$ GeV and $\theta_n/\pi \in [0, 0.5]$ divided into 20 equally-spaced bins (linearly for θ_n and logarithmically for E), for a total of 400 bins for cascade events and an equal number for track events.

In the analysis δ and $\sin^2\theta_{23}$ are kept fixed to certain values. We have obtained results for $\delta = 3\pi/2$ and eleven values of $\sin^2\theta_{23}$ from the interval [0.40,0.60], which belong to, and essentially span, the 3σ range of allowed values of $\sin^2\theta_{23}$ obtained in the latest global neutrino data analyses.

The statistical analysis of ORCA event distributions is performed employing the χ^2 method described in arXiv:1503.01999.

In the analysis we included, in addition to the statistical uncertainties, four sets of systematic uncertainties: minimal, optimistic, default and conservative.

More specifically, we include the following set of systematic uncertainties:

i) oscillation and normalization uncertainties, where the latter include an overall normalization error (15%), as well as the relative ν_μ/ν_e and $\nu/\bar{\nu}$ flux uncertainties (8% and 5%, respectively);

ii) energy-scale (5%) and energy-angle resolution uncertainties (10%), independently for cascade and track events;

iii) energy-angle spectral shape uncertainties, via quartic polynomials in both θ_n and E. These are meant to characterize systematic effects including: uncertainties in the primary cosmic ray fluxes, differential atmospheric neutrino fluxes and cross sections and, to some extent, energy-angle detection efficiencies;

iv) residual uncorrelated systematics in each bin, representing the presence of unknown uncertainties, like those coming from a finite Monte Carlo statistics in experimental simulations.

We define as "minimal" set of systematics the one including only those described in point i) in the preceding list.
When we add the uncertainties at point ii), iii) and iv), assuming a prior of 0.75% (1.5%) on the coefficients of the quartic polynomials and a 0.75% (1.5%) uncorrellated error in each bin, we obtain our "optimistic" set ("default" set).
Finally, if we instead consider a 3% uncertainty on polynomial coefficients and uncorrelated errors we get our "conservative" set. All the systematics mentioned above are implemented using the pull method.

Results

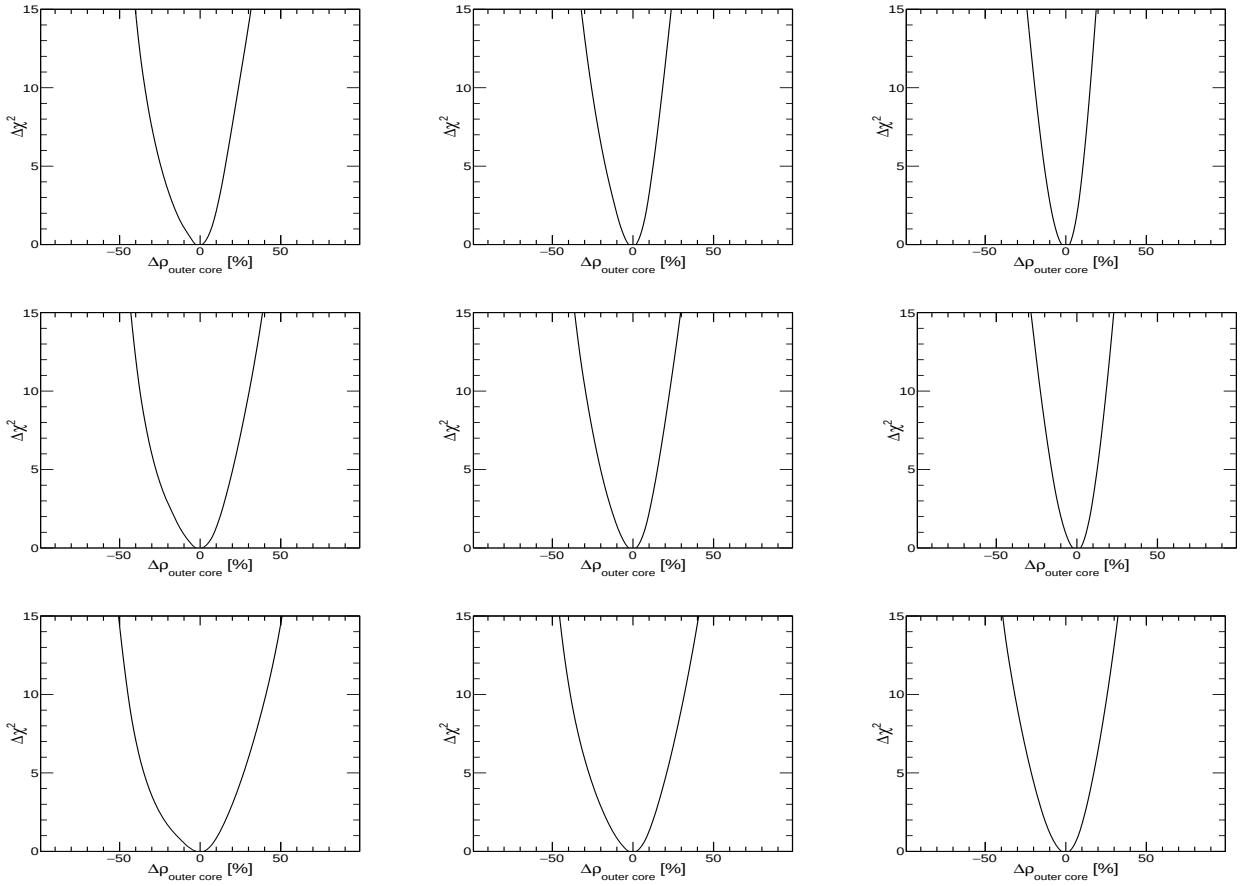

Figure 1: Sensitivity to the OC density in the case of NO spectrum and 10 years of data. The Earth total mass constraint is implemented by compensating the OC density variation with a corresponding mantle density change. The results shown are for $\sin^2\theta_{23} = 0.42,\ 0.50,\ 0.58$ (left, center and right panels) and in the cases of "minimal", "optimistic" and "conservative" systematic errors (top, middle and bottom panels). See text for further details.

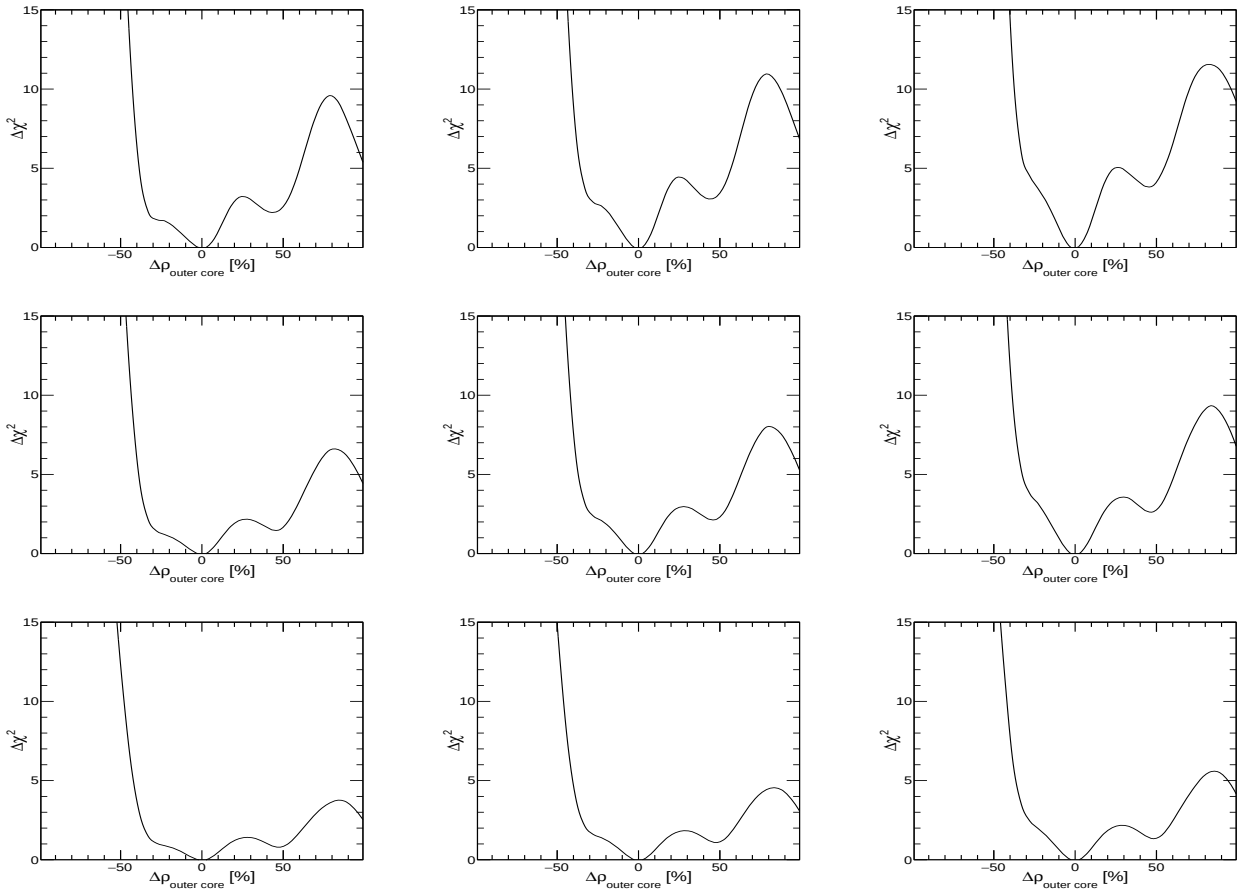

Figure 3: The same as in Fig. 1, but without implementing the Earth total mass constraint. The results shown are for $\sin^2\theta_{23} = 0.42,\ 0.50,\ 0.58$ (left, center and right panels) and in the cases of "minimal", "optimistic" and "conservative" systematic errors (top, middle and bottom panels). See text for further details.

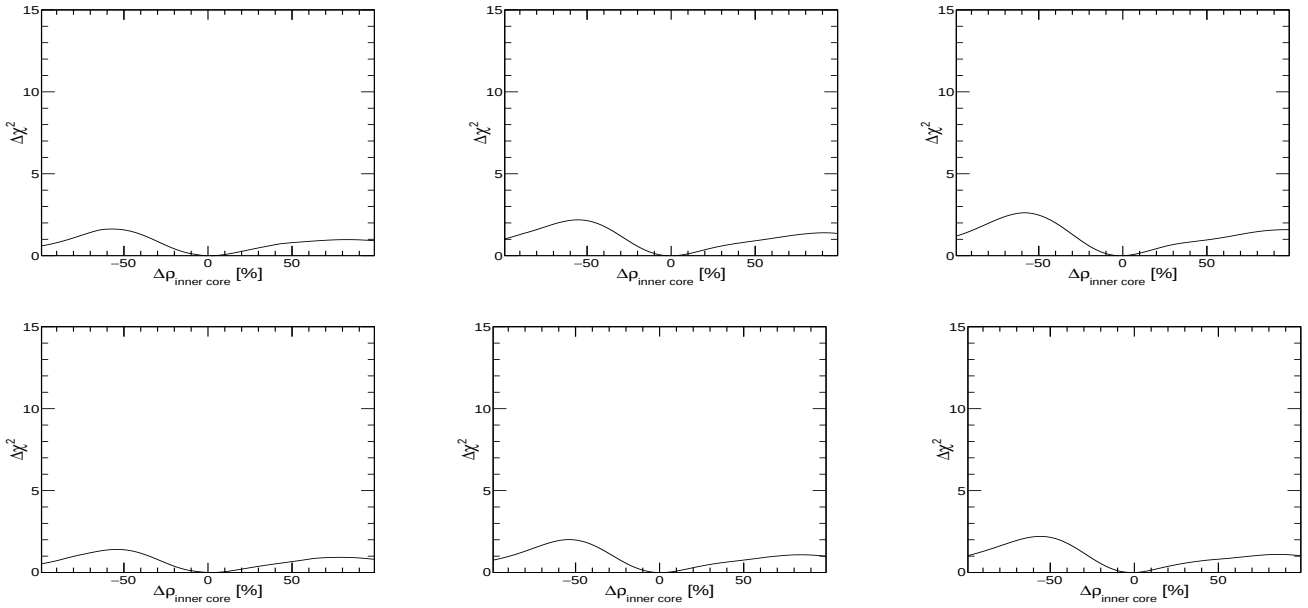

Figure 4: Sensitivity to the IC density. The Earth total mass constraint i) is implemented by compensating the IC density variation with a corresponding mantle density change (top panels), ii) is not implemented (bottom panels). The results shown are for $\sin^2\theta_{23} = 0.42$, 0.50, 0.58 (left, center and right panels) and in the case of "minimal" systematic errors. See text for further details.

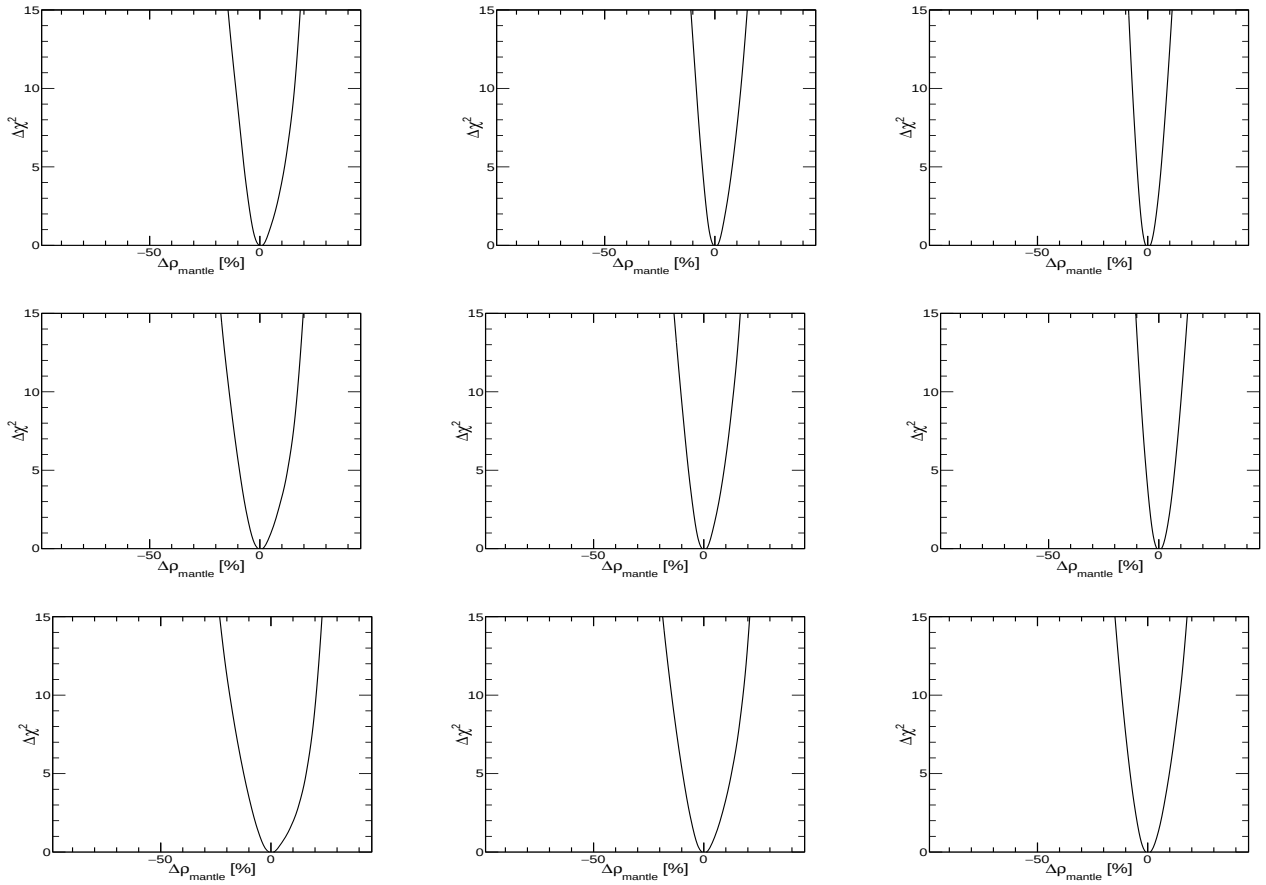

Figure 7: Sensitivity to the mantle density in the case of NO spectrum and 10 years of data. The Earth total mass constraint is implemented by compensating the mantle density variation with a corresponding OC density change. The results shown are for $\sin^2\theta_{23} = 0.42$, 0.50, 0.58 (left, center and right panels) and in the cases of "minimal", "optimistic" and "conservative" systematic errors (top, middle and bottom panels). See text for further details.

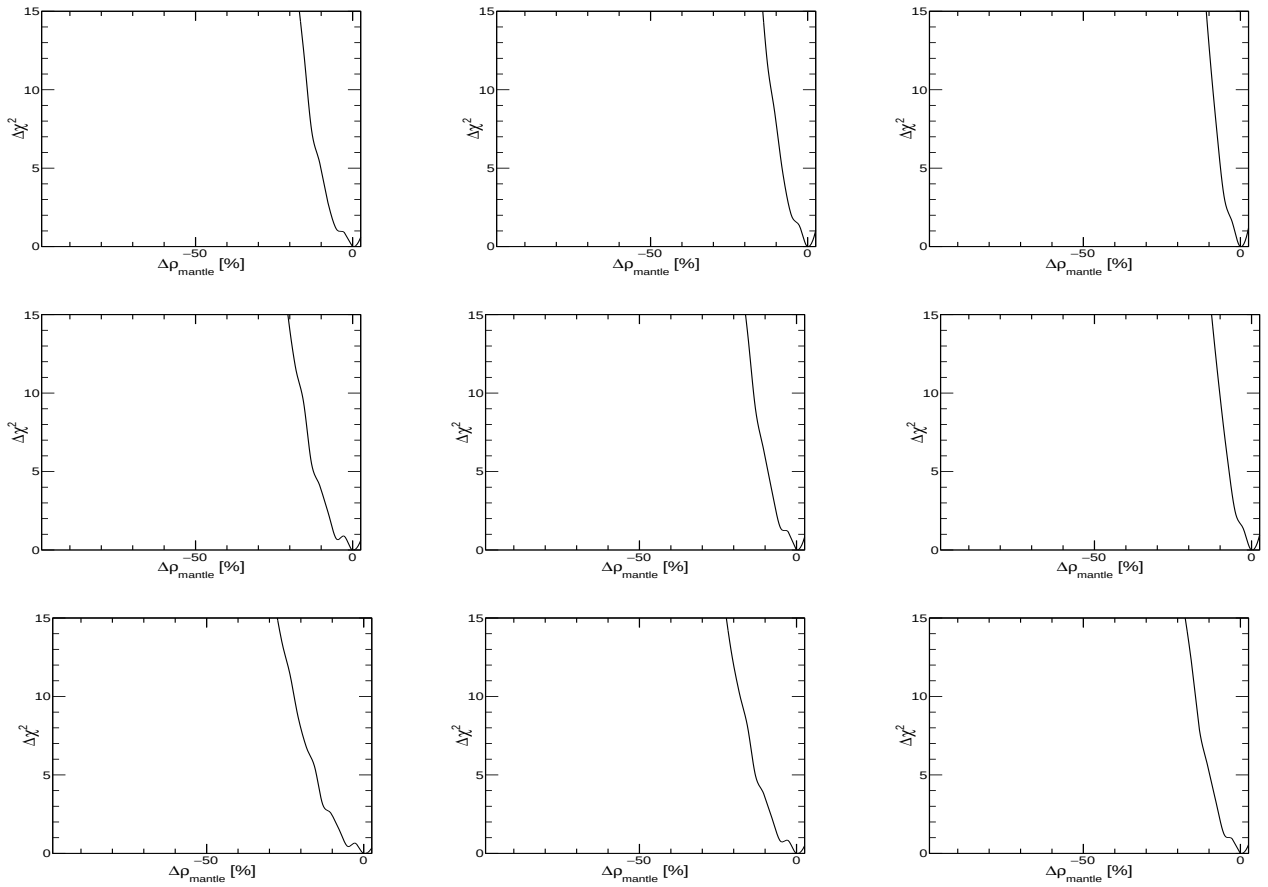

Figure 8: The same as in Fig. 7, but with implementing the Earth total mass constraint by compensating the mantle density variation with a corresponding IC density change. The results shown are for $\sin^2\theta_{23} = 0.42$, 0.50, 0.58 (left, center and right panels) and in the cases of "minimal", "optimistic" and "conservative" systematic errors (top, middle and bottom panels). See text for further details.

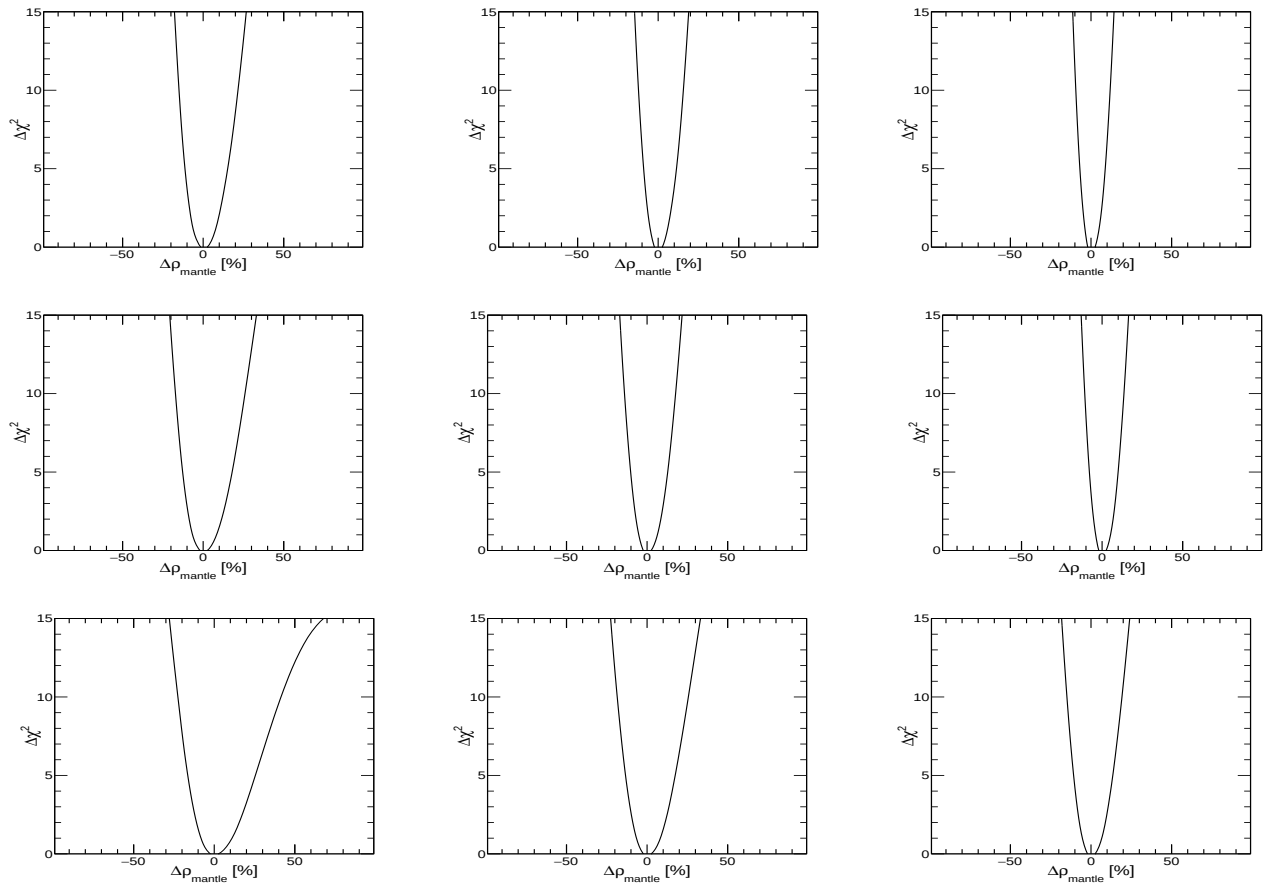

Figure 9: The same as in Fig. 7, but without implementing the Earth total mass constraint. The results shown are for $\sin^2\theta_{23} = 0.42,\ 0.50,\ 0.58$ (left, center and right panels) and in the cases of "minimal", "optimistic" and "conservative" systematic errors (top, middle and bottom panels). See text for further details.

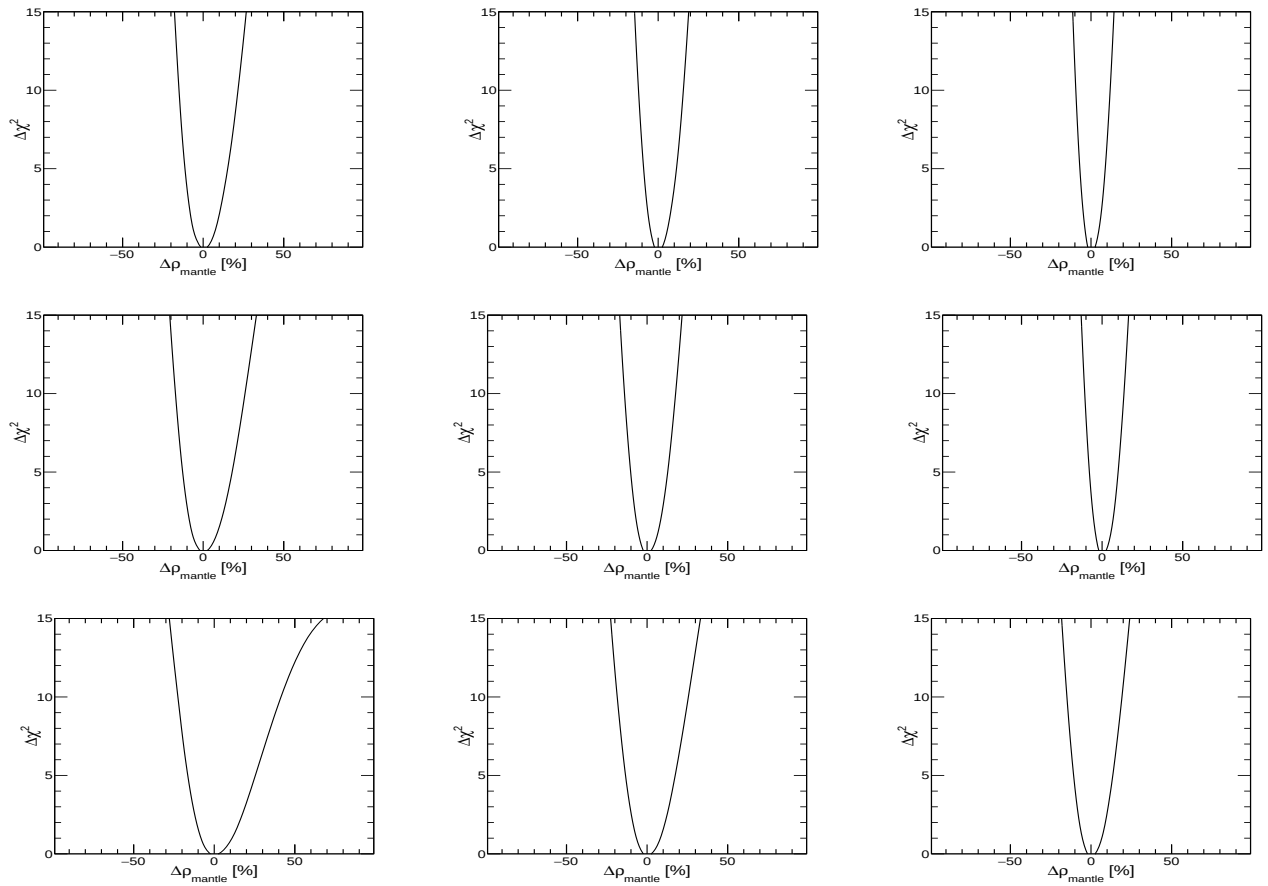

Figure 9: The same as in Fig. 7, but without implementing the Earth total mass constraint. The results shown are for $\sin^2\theta_{23} = 0.42,\ 0.50,\ 0.58$ (left, center and right panels) and in the cases of "minimal", "optimistic" and "conservative" systematic errors (top, middle and bottom panels). See text for further details.

The sensitivity of ORCA to the densities of the outer core, core and mantle depend strongly
1. on the value of $\sin^2\theta_{23}$,
2. on the type of systematic errors employed in the analysis,
3. on whether the total Earth mass constraint is implemented or not, and
4. on the way the compensation of the density variation in a given layer by a change of density in another layer is implemented, i.e., on the choice of the "compensating" layer, when the total Earth mass constraint is imposed.

It depends also strongly on the type of neutrino mass spectrum.

"Most favorable" NO case: of "minimal" systematic errors, $\sin^2\theta_{23} = 0.58$ and implemented Earth mass constraint, ORCA can determine, e.g., the OC density with mantle serving as a compensation layer at 3σ C.L. after 10 years of operation with uncertainty of
(-18%)/+12%.
Similarly, ORCA can determine the mantle density using OC as a "compensating" layer with uncertainty of (-6%)/+8%).

In the "most disfavorable" NO case with implemented Earth mass constraint but "conservative" systematic errors and $\sin^2\theta_{23} = 0.42$, these uncertainties read (-43%)/+39% and (-17)%/+20%;
for $\sin^2\theta_{23} = 0.50$, 0.58 they are noticeably smaller:
(-37)%/+30%, (-30%)/+24% and (-13%)/+17%, (-11%)/+14%).

The Earth Hydrostatic Equilibrium (EHE) constraints were taken into account and there effects were accounted for; in certain cases results remain unchanged, in other cases they change somewhat, but not dramatically.

In the case of OC (mantle) density variation compensated by a change of the mantle (OC) density, the EHE constraints imply approximately:
$(-49.6\%) \lesssim \Delta\rho_{\text{outer core}} \lesssim 18.3\%$ **(**$(-8.3\%) \lesssim \Delta\rho_{mantle} \lesssim 22.8\%$**).**

In what concerns the derived ORCA 3σ **sensitivity ranges of** $\Delta\rho_{\text{outer core}}$ **reported above,**
i) the lower limit of (-49.6%) from the EHE constraints has no effect on them,
ii) the effects of the upper limit of 18.3%, if any, depends on $\sin^2\theta_{23}$ **and on the type of implemented systematic errors.**

The upper limit of 18.3% has no effect on the ORCA 3σ **sensitivity ranges in the case of "minimal" systematic errors for any** $\sin^2\theta_{23} \gtrsim 0.50$**;**
for $\sin^2\theta_{23} = 0.42$**, it corresponds to the maximal value of the ORCA** 2σ **sensitivity range.**
Fot the set of "optimistic" systematic errors, 18.3% represents approximately the maximal value of the 2σ**,** 2.4σ **and** 2.6σ **ORCA sensitivity ranges for** $\sin^2\theta_{23} = 0.50$**, 0.54 and 0.58, respectively.**
The effect of the discussed constraint is largest for the ORCA sensitivity ranges obtained with conservative systematic errors:

18.3% corresponds, e.g., to the maximal value of the ORCA 1.9σ sensitivity range at $\sin^2\theta_{23} = 0.58$.

In a similar way, the RHE constraints do not restrict from above the reported ORCA 3σ sensitivity to $\Delta\rho_{mantle}$ even in the case of "conservative" systematic errors.
The maximal allowed negative variation of (-8.3%) restricts from below the ORCA sensitivity ranges.
For example, in the case of "minimal" systematic errors, $\Delta\rho_{\text{mantle}} = -8.3\%$ corresponds to the minimal values of the ORCA 2σ, 2.4σ, 2.8σ and 3.0σ sensitivity ranges derived for $\sin^2\theta_{23} = 0.46$, 0.50, 0.54 and 0.58, respectively.

With maximally reduced systematic errors and certain further improvements, e.g., the discussed "favorable" 6 m vertical spacing configuration of ORCA experiment or the Super-ORCA version of the detector the ORCA sensitivities to positive $\Delta\rho_{\text{outer core}}$ (negative $\Delta\rho_{\text{mantle}}$) might increase sufficiently so that the EHE constraint $\Delta\rho_{\text{outer core}} \lesssim 18.3\%$ ($(-8.3\%) \lesssim \Delta\rho_{\text{mantle}}$) would have no effect on the ORCA 3σ sensitivity to positive variations of ρ_{OC} compensated by changes of ρ_{mantle} (negative variations of ρ_{mantle} compensated by changes of ρ_{OC}).

The uncertainties in the determination of the outer core, total core and mantle densities by ORCA in the case of NO spectrum, according to our results, are considerably larger if the total Earth mass constraint is not implemented in the analysis, or if it is implemented but the inner core is used as a "compensation" layer.

We find also that the sensitivity of ORCA to the outer core, core and mantle densities is significantly worse for the IO neutrino mass spectrum than for the NO spectrum.

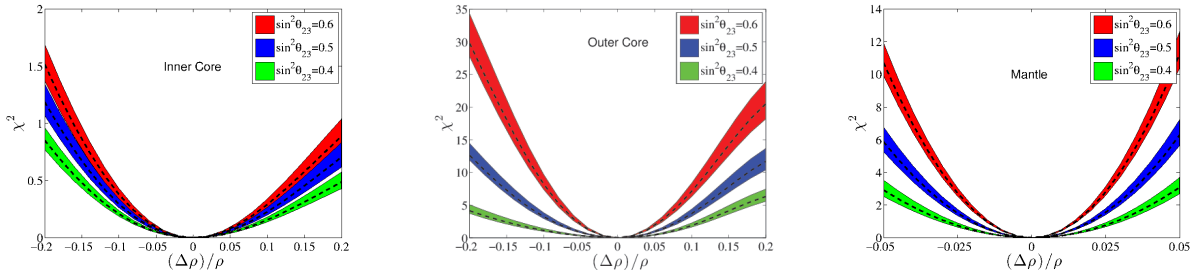

Figure 11: PINGU prospective sensitivity to the inner core (left panel), outer core (middle panel) and mantle (right panel) densities in the case of NO spectrum and 10 years of data. The ratios $\Delta\rho/\rho$ in the three panels correspond respectively to $\Delta\rho_{\text{inner core}}$, $\Delta\rho_{\text{outer core}}$ and $\Delta\rho_{\text{mantle}}$ defined in the main text. The results shown are for $\sin^2\theta_{23} = 0.40, 0.50, 0.60$. The bands correspond to variation of $\sin^2\theta_{13}$ in the interval 0.020 - 0.025 and marginalisation over θ_{23}, Δm^2_{31} and θ_{13}. (Figures from S. Choubey and S.T. Petcov, studies performed in 2014, unpublished .)

Conclusion.

The neutrino tomography of the Earth is a promissing powerful alternative method of obtaining valuable information about the Earth interior. It is at initial stage of development.

The ORCA experiment has the potential of making unique pioneering contributions to the studies of the Earth interior with atmospheric neutrinos, i.e., to the neutrino tomography of the Earth.